Journal of Atmospheric and Terrestrial Physics, Vol. 53, No. 11/12, pp. 1005–1018, 1991.
Printed in Great Britain.

0021–9169/91 $3.00 + 00
Pergamon Press plc

Revised solar extreme ultraviolet flux model

W. KENT TOBISKA

Earth and Planetary Atmospheres Group/Space Sciences Laboratory, University of California, Berkeley, CA 94720, U.S.A.

(*Received in final form* 22 *April* 1991)

Abstract—An extended and revised solar extreme ultraviolet irradiance model for aeronomical use during the 1990s has been developed. The extensions significantly increase the application of the SERF2 solar EUV model beyond the October 1981–April 1989 time-frame. The model can now be used from 1947 to the present for coronal EUV full-disk irradiances and from 1976 to the present for chromospheric EUV full-disk irradiances. Substantial revisions to SERF2 were made which significantly improve the ability of the model to reproduce observed 27-day and solar cycle EUV temporal variations. A multiple linear regression method is used to obtain coefficients for modelled EUV photon flux. This method allows for the inclusion of new rocket and satellite datasets into the model as they become available. The solar H Lyman-α and He I 10,830 Å equivalent width measurements are used as the independent model parameters for the chromospheric irradiances while the 10.7-cm radio emission daily and 81-day running mean values are the independent parameters for the coronal and transition region irradiances. The results of the model give full-disk photon fluxes at 1 AU for 39 EUV wavelength groups and discrete lines between 1.8 and 105.0 nm for a given date. The OSO, AEROS, AE satellite datasets and six rocket datasets used in the model development are summarized, the modelling technique is described in detail, the model formulation is presented, and the comparisons of the model to the datasets are discussed.

INTRODUCTION

Solar extreme ultraviolet (EUV) radiation which is emitted between the X-rays and the far ultraviolet is a combination of both line and continuum features. Its importance results from this spectrum's relationship with planetary thermospheres which are heated by EUV radiation through photoabsorption processes. For example, the Earth's upper atmosphere is significantly perturbed by this irradiance which is absorbed by the major neutral constituents of O, O_2, and N_2.

SCHMIDTKE (1984) outlined four aeronomically important solar spectral ranges. The 125.0–180.0 nm range heats the lower thermosphere through the production of O by O_2 absorption in the Schumann-Runge continuum; the H Lyman-α line at 121.6 nm is a major contributor of the *D*-region ionosphere through the ionization of NO; the 16.0–103.0 nm range is the primary heat source of the thermosphere through major neutral constituent photoabsorption and creates the ionosphere *E*- and *F*-regions; and the 0.1–2.0 nm range contributes to the ionization of the *D*-region, particularly during active solar conditions. For a detailed understanding of the temporal variations of the thermosphere over solar rotation and solar cycle time scales, the temporal variations of the 2–103 nm range are of particular interest.

The EUV irradiances between 1.8 nm and H Lyman-α have been measured by numerous sounding rocket and satellite instruments. These measurements have been reviewed by TIMOTHY (1977), SCHMIDTKE (1981, 1984), and LEAN (1987). Further rocket measurements have been described by CARLSON *et al.* (1984), OGAWA and JUDGE (1986), OGAWA *et al.* (1990), WOODS and ROTTMAN (1990), and summarized by FENG *et al.* (1989). In essence, these papers describe over a dozen and a half sounding rocket measurements and measurements by the OSO, AEROS, and AE series satellites using both spectrophotometric and broadband ionization cell techniques during the 1960s to the 1980s.

These measurements have provided a wealth of information on the relative temporal variation of many line and continuum emission features in this spectral range. Important periodicities were discovered in the long-term solar cycle EUV variation and the ranges of absolute intensities within which these features vary were established. As such, these measurements laid the groundwork for solar EUV models which are used when measurements are unavailable.

Prior to measurements above the atmosphere, the first empirical EUV model can be found in the 1937 suggestion of SAHA (1937) that an 'ultraviolet excess factor' be accounted for by scaling the EUV spectral region in a solar black body radiating at 6500 K by 1×10^6. Following a successful rocket observation

of a broad spectrum in the EUV during 1963, HINTEREGGER *et al.* (1965) tabulated an EUV flux standard for quiet solar conditions. This was followed by the compilation by DONNELLY and POPE (1973) of an EUV model spectrum for moderate solar activity which summarized the subsequent successful observations. HINTEREGGER (1976) reviewed the advances in measuring EUV irradiances following the Atmospheric Explorer-C (AE-C) mission in the mid-1970s and HEROUX and HINTEREGGER (1978) released a revised reference spectrum for moderate solar activity based upon a detailed study of a 1974 rocket flight. ROBLE and SCHMIDTKE (1979) described a variety of typical EUV flux examples applied to aeronomical calculations for different solar conditions.

However, the most complete empirical models were first developed by HINTEREGGER *et al.* (1981) following the completion of the AE-E mission. Two empirical models emerged from this work including the EUV class model and the two variable 10.7 cm radio flux, $F_{10.7}$, association formula. The EUV class model was limited to the time-frame of the AE-E mission (July 1977–December 1980) and used the chromospheric H Lyman-β flux to estimate other chromospheric emission intensities and used the Fe XVI (33.5 nm) coronal line to estimate other coronal and transition region (hereafter referred to as coronal) emission intensities. The association formula used both $F_{10.7}$ daily and 81-day mean values in a linear correlation with AE-E EUV flux values in order to estimate EUV irradiances outside that time-frame. These combined models were later designated SERF1 by the Solar Electromagnetic Radiation Flux Study group which worked under the auspices of the World Ionosphere–Thermosphere Study (WITS) organized by the Scientific Committee on Solar-Terrestrial Physics (SCOSTEP).

Following the SERF1 model, TOBISKA (1988) developed a two index EUV flux model based on the HINTEREGGER *et al.* (1981) EUV class model concept and the AE-E dataset. This model used H Lyman-α to estimate the chromospheric irradiances and 0.1–0.8 nm X-rays to estimate the coronal irradiances. TOBISKA and BARTH (1990) improved this model by replacing the 0.1–0.8 nm X-ray index with the $F_{10.7}$ daily values and by utilizing additional, mostly broadband, rocket measurements of the EUV to lower the uncertainty on the absolute integrated irradiance values. This model was subsequently designated SERF2 and covered the time-frame between October 1981 and April 1989. TOBISKA (1990) detailed the SERF2 model development.

SERF1 and SERF2 were compared by LEAN (1990) over time-scales of the 27-day solar rotation and the 11-year solar cycle. Significant differences were found between the two models and between the models and the datasets upon which each were based. The differences appeared in the estimation of absolute intensities, the magnitude of peak-to-valley variation of irradiance due to solar rotation, and the maximum to minimum flux values over the 11-year solar cycle. The conclusion of that study indicated neither models nor measurements yet provided a consistent picture of long-term variability in the EUV portion of the Sun's spectrum.

The revisions and extension of the SERF2 model in the present study are part of the continuing effort to improve empirical solar EUV modelled irradiances such that the uncertainties are better known in both models and datasets and such that the models become a useful tool for estimating solar EUV irradiance for aeronomical use.

EUV MODEL DEVELOPMENT

SERF2 improvements

SERF2 represented an advance for empirical solar EUV irradiance modelling based upon (1) the extension of the EUV class method to time periods outside of the AE-E dataset and (2) the high correlations of the Lyman-α and $F_{10.7}$ proxies with the AE-E chromospheric and coronal irradiances, respectively. However, a detailed analysis of the model identified the following inconsistencies and limitations. Two of the inconsistencies are apparent when the model is directly compared to datasets and one subtle physical inconsistency was discovered. A significant limitation of SERF2 resulted from its application only to the 1981–1989 time-frame.

TOBISKA (1990) and LEAN (1990) both indicated that several of the SERF2 chromospheric lines, including the He I 58.4 nm, He II 30.4 nm, and the H Lyman-β 102.6 nm features, did not show large enough relative amplitude variation over 27-day solar rotation time scales when compared to OSO 4, OSO 6, and AE-E datasets. In addition, there was a concern that the absolute magnitudes of these particular lines were too low and that the ratios of solar cycle maximum to minimum values were too low. It was later determined that the method of weighting the slope coefficient rather than the intercept in the SERF2 linear equations was the most probable cause of this inconsistency. This subsequently raised concerns about the overall usefulness of this weighting method.

A second concern raised about the SERF2 model was its use of the daily $F_{10.7}$ value, but not the 81-day

mean value, combined with an H Lyman-α proxy in estimating the coronal irradiances. The $F_{10.7}$ 81-day mean value used by SERF1 has been recognized as a way of improving the $F_{10.7}$ and EUV emission correlations, particularly for coronal emissions.

A third concern about the model was pointed out by LINK [private communication (1990)] who demonstrated that SERF2 did not reproduce physically consistent H Lyman and C I continua. The 5.0 nm wavelength interval boundaries in the SERF2 modelled continuum flux were not consistent in magnitude with the neighbouring continuum interval.

An open question which was addressed by SERF2 and which still remains to be resolved is the debate on whether or not the 5.0–57.5 nm total integrated flux for low solar activity should be higher than the irradiances measured by rockets in the 1970s. RICHARDS and TORR (1984), OGAWA and JUDGE (1986), LINK *et al.* (1988), WINNINGHAM *et al.* (1989), and TOBISKA (1989) indicate that the estimates of some or all of the total flux in that wavelength range should be higher during low solar activity by up to a factor of 2. SERF2 produced total integrated flux of about 1.6 greater than the rocket data. The present model produces total 5.0–57.5 nm integrated flux values which match the rocket data. However, in the subrange of 5.0–25.0 nm, the model consistently produces higher flux for all levels of solar activity than the AE-E data. This result supports the conclusions of RICHARDS and TORR (1984) who determined that a doubling of the solar EUV below 25.0 nm was needed to explain measured photoelectron fluxes. This issue will be addressed later in the evaluation of this new model.

Datasets used in the model development

Six satellite EUV datasets, including OSO 1 (28.4 and 30.4 nm), OSO 3 (25.6, 28.4, and 30.4 nm), OSO 4 (30.4 nm), OSO 6 (30.4 and 58.4 nm), AEROS A (28.4, 30.4, and 58.4 nm), and AE-E (14.0–105.0 nm), were used in the development of this model. Each dataset was weighted for instrument uncertainty. These EUV data were combined with data from six rocket flights, also weighted, to obtain the irradiances at EUV wavelengths for correlation with the model proxies. The six rockets included three ionization cell or silicon photodiode instruments flown by the University of Southern California and described by CARLSON *et al.* (1984), OGAWA and JUDGE (1986), and OGAWA *et al.* (1990), two spectrographs flown by the University of Colorado described by WOODS and ROTTMAN (1990) and WOODS [private communication (1991)], and one spectrometer flown by the Air Force Geophysics Laboratory described by VAN TASSEL *et al.* (1981). Table 1 lists the characteristics of these datasets by satellite, wavelength coverage, year(s) of observations, literature reference, and uses in model development.

The model proxies, which are independent datasets used to establish a correlation between either chromospheric or coronal irradiances or to extend the estimate of these irradiances outside the original EUV data time-frames, include the Solar Mesosphere Explorer (SME) Lyman-α described by BARTH *et al.* (1990), the AE-E Lyman-α described by HINTEREGGER *et al.* (1981), the OSO 4 Lyman-α described by TIMOTHY and TIMOTHY (1970), the OSO 6 Lyman-α described by WOODGATE *et al.* (1973), the He I 10,830 Å equivalent width (EW) described by HARVEY (1984), and the Ottawa $F_{10.7}$ provided by the World Data Center A.

Modelling technique and formulation

The revision and extension of the SERF2 model was conducted using a multiple linear regression technique which is different from the simple least squares fitting routine used to develop the original SERF2 model. The advantage of using a multiple linear regression algorithm in this new model is that several datasets from independent sources may be used to perform the new correlations. With the number of independent terms greater than 1 for each of the chromospheric and coronal regressions, the new model (1) is now capable of including new proxies to extend the model backward or forward in time (as has been done with the He I 10,830 Å EW data) or (2) is now able to take advantage of higher correlations obtained with mean value data (as has been done with the 81-day mean of the $F_{10.7}$). Additionally, future independent datasets which prove to have high correlations with solar chromospheric or coronal irradiances can now be included. The weighting of the datasets is easily accomplished using the multiple linear regression algorithm.

In general, a chromospheric or coronal emission intensity, I, at a wavelength λ may be modelled as a time-varying quantity at 1 AU as

$$I(\lambda, t) = a_0(\lambda) + a_1(\lambda)F_1(t) + a_2(\lambda)F_2(t) + \cdots + a_n(\lambda)F_n(t) \quad (1)$$

in units of photons $cm^{-2} s^{-1}$ with n independent terms according to the multiple linear regression technique described by BEVINGTON (1969). The $a_i(\lambda)$ coefficients are derived in the multiple linear regression and $F_n(t)$ are the independent datasets ($n = 4$ for the model) which are the EUV proxies as used in this study.

Table 1. Datasets used for the solar EUV model

Dataset	λ*	Time-frame	Reference	Comments
OSO 1	284, 304	1962	NEUPERT *et al.* (1964)	EUV: Used ±35% uncertainty
OSO 3	256, 284, 304	1967	CHAPMAN and NEUPERT (1974)	EUV: Used ±35% uncertainty
OSO 4	304	1967–69	TIMOTHY and TIMOTHY (1970)	EUV: Used ±35% uncertainty
OSO 4	1216	1967–69	TIMOTHY and TIMOTHY (1970)	H Lyα: Used as a proxy
OSO 6	304, 584	1969	WOODGATE *et al.* (1973)	EUV: Used ±35% uncertainty
OSO 6	1216	1969	WOODGATE *et al.* (1973)	H Lyα: Used as a proxy
AEROS A	284, 304, 584	1972	SCHMIDTKE *et al.* (1977)	EUV: Used ±35% uncertainty
AE-E	140–1050	1977–80	HINTEREGGER *et al.* (1981)	EUV: Used ±35% uncertainty
AE-E	1216	1977–78	HINTEREGGER *et al.* (1981)	H Lyα: Used as a proxy
AFGL	18–140	1979	VAN TASSEL *et al.* (1981)	EUV: Used ±35% uncertainty
USC	50–575	1982	CARLSON *et al.* (1984)	EUV: estimated using scaled AFGL (±55%)
USC	50–575	1983	OGAWA and JUDGE (1986)	EUV: estimated using scaled AFGL (±55%)
USC	50–575	1988	OGAWA *et al.* (1990)	EUV: estimated using scaled AFGL (±55%)
LASP	300–1050	1988	WOODS and ROTTMAN (1990)	EUV: λ variable uncertainty (±10–60%)
LASP	350–1050	1989	WOODS (private comm., 1991)	EUV: λ variable uncertainty (±12–80%)
SME	1216	1981–89	BARTH *et al.* (1990)	H Lyα: Used as a proxy
NSO	10,830 EW	1975–89	HARVEY (1984)	He I 10,830 Å EW: Used as a proxy
WDC A	10.7 cm	1947–89	COVINGTON (1948) and WDC A	$F_{10.7}$: Used as a proxy

* Wavelengths in Å except the 10,830 equivalent width and 10.7 cm flux datasets.

This relationship is based on the assumption that the independent terms vary linearly with the EUV flux with which they are being correlated. The assumption generally holds true for emissions which are created at the same temperature levels in the solar atmosphere.

This equation is modified to reproduce modelled flux during periods when one of the independent terms, or proxies, may not be available. A good example of this is between the end of AE-E in December 1980 and the start of SME in October 1981. During these 9 months, there were no Lyman-α data measured although He I 10,830 Å EW measurements do exist. Therefore, an empirical function was developed to allow the production of the modelled flux even if one independent term is missing. This function has the dimensionless form

$$w_i(\lambda, t) = 1 + b_i(\lambda)\, e^{-S_i(t)} \tag{2}$$

$$W(\lambda, t) = \prod_{i=1}^{4} w_i(\lambda, t) \tag{3}$$

where the $w_i(\lambda, t)$ scaling term corresponds to the average ratio by which the $F_j(t)$ independent term is multiplied in order to model the flux for the days which have missing data in the ith independent term. $S_i(t)$ is a step function which has a large value ($\gg 1$) for dates on which data exist for the ith independent term and a value of 0 for dates on which data do not exist for the ith independent term. In the exponent, $-S_i(t)$ causes $b_i(\lambda)$ to be multiplied by 0 or 1 for data or no data, respectively, in the ith independent term. If the ith independent term data exist for a given date, the value of $w_i(\lambda, t)$ reduces to unity. In practice, an equally valid alternative to using the weighting function is to set $w_i(\lambda, t)$ to 1 and scale an existing proxy from the same solar temperature region to the value of the missing proxy on a given date.

Equation (1) can now be rewritten as

$$\Phi(\lambda, t) = a_0(\lambda) + \sum_{i=1}^{4} a_i(\lambda) F_i(t) \tag{4}$$

$$I(\lambda, t) = \Phi(\lambda, t)\, W(\lambda, t) \tag{5}$$

again in units of photon flux.

In the model, there are presently four independent datasets used where $F_1(t)$ is the SME Lyman-α, $F_2(t)$ is the He I 10,830 Å EW scaled to Lyman-α values by equation (6) below, $F_3(t)$ is the daily $F_{10.7}$, and $F_4(t)$ is the 81-day running mean value of $F_{10.7}$. If the modelled flux is chromospheric in origin, then the coefficients of $a_3(\lambda)$ and $a_4(\lambda)$ are set to 0 or if the flux is coronal in origin, then the coefficients of $a_1(\lambda)$ and $a_2(\lambda)$ are set to 0. For wavelength intervals in which both chromospheric and coronal irradiances are modelled, each interval is calculated separately according to chromospheric or coronal classification with the final values then summed in order to produce a total flux for that particular wavelength interval.

Table 2 lists coefficients used in the model by 39 wavelength intervals or discrete lines and includes the solar source region (key) for each EUV wavelength, the value of $a_0(\lambda)$ in equation (4), the values of $a_i(\lambda)$ for $i = 1, 2, 3, 4$ in equation (4), and the values of $b_i(\lambda)$ for $i = 1, 2, 3, 4$ in equation (2). These intervals and lines are identical to the divisions made in previous EUV investigations by TORR *et al.* (1979), TORR

Table 2. Solar EUV model coefficients

λ_1	λ_2	Key*	a_0	a_1	a_2	a_3	a_4	b_1	b_2	b_3	b_4
18	30	2	−3.41318e+07	0	0	313454.	203595.	0	0	0	0
31	50	1	−1.09355e+07	−7.94382e−07	9.08989e−05	0	0	0	0	0	0
31	50	2	−6.09718e+07	0	0	550330.	357449.	0	0	0	0
51	100	1	−2.63824e+08	−1.91867e−05	0.00219300	0	0	0	0	0	0
51	100	2	−2.01169e+08	0	0	3.59384e+06	2.32841e+06	0	0	0	0
101	150	1	−1.04138e+08	−8.22424e−06	0.000891052	0	0	0	0	0	0
101	150	2	−2.10080e+05	0	0	634184.	409793.	0	0	0	0
151	200	1	−1.74864e+08	−1.80512e−05	0.00206329	0	0	0	0	0	0
151	200	2	−8.50452e+08	0	0	2.15983e+07	1.39840e+07	0	0	0	0
201	250	1	−2.03915e+08	−2.09982e−05	0.00240001	0	0	0	0	0	0
201	250	2	−1.89626e+09	0	0	2.02855e+07	1.31572e+07	0	0	0	0
256	256	1	1.38842e+07	−1.46978e−05	0.00168003	0	0	0	0	0	0
284	284	2	−1.59676e+09	0	0	1.60441e+07	9.43640e+06	0	0	0	0
251	300	1	−7.71343e+07	−1.50827e−05	0.00172379	0	0	0	0	0	0
251	300	2	−3.82102e+09	0	0	3.48145e+07	2.27244e+07	0	0	0	0
303	303	2	−1.05822e+09	0	0	1.00705e+07	7.17696e+06	0	0	0	0
304	304	1	2.13752e+08	−0.000226291	0.0258646	0	0	0	0	0	0
301	350	2	−4.65860e+09	0	0	4.45973e+07	2.91061e+07	0	0	0	0
368	368	2	2.87050e+08	0	0	2.79581e+06	1.72142e+06	0	0	0	0
351	400	1	−5.81541e+06	−1.12337e−06	0.000128456	0	0	0	0	0	0
351	400	2	−1.12033e+09	0	0	1.72024e+07	1.10261e+07	0	0	0	0
401	450	1	−5.89502e+07	−1.22128e−05	0.00132439	0	0	0	0	0	0
401	450	2	−1.06976e+08	0	0	2.80860e+06	1.75990e+06	0	0	0	0
465	465	2	5.89122e+07	0	0	844715.	520445.	0	0	0	0
451	500	1	−1.97061e+08	−1.56238e−05	0.00169281	0	0	0	0	0	0
451	500	2	−6.34740e+08	0	0	7.16843e+06	4.63953e+06	0	0	0	0
501	550	1	−4.19715e+08	−4.59571e−05	0.00497787	0	0	0	0	0	0
501	550	2	−3.71313e+08	0	0	3.55929e+06	2.21819e+06	0	0	0	0
554	554	1	−7.97548e+07	−2.02374e−05	0.00219424	0	0	0	0	0	0
584	584	1	−2.40495e+09	−0.000153653	0.0175749	0	0	0	0	0	0
551	600	1	−1.46516e+09	−0.000121477	0.0131716	0	0	0	0	0	0
610	610	2	−2.41248e+08	0	0	5.22489e+06	2.80106e+06	0	0	0	0
630	630	1	−3.35132e+08	−6.93450e−05	0.00793129	0	0	0	0	0	0
601	650	1	−2.40639e+08	−5.17362e−05	0.00560399	0	0	0	0	0	0
601	650	2	−1.76203e+08	0	0	3.64330e+06	2.32576e+06	0	0	0	0
651	700	1	−1.27308e+08	−1.53857e−05	0.00166689	0	0	0	0	0	0
651	700	2	4.86650e+07	0	0	331301.	189074.	0	0	0	0
703	703	1	−2.33824e+07	−1.34269e−05	0.00145498	0	0	0	0	0	0
701	750	1	−6.59055e+07	−1.03401e−05	0.00112006	0	0	0	0	0	0
765	765	1	−9.70166e+07	−1.18976e−05	0.00128858	0	0	0	0	0	0
770	770	2	−3.39939e+07	0	0	1.75960e+06	1.12721e+06	0	0	0	0
788	790	1	−1.44843e+08	−3.41136e−05	0.00390135	0	0	0	0	0	0
751	800	1	−4.03383e+08	−4.75317e−05	0.00514966	0	0	0	0	0	0
751	800	2	−4.63681e+07	0	0	2.18818e+06	1.39238e+06	0	0	0	0
801	850	1	−1.91195e+09	−0.000152746	0.0165448	0	0	0	0	0	0
851	900	1	−6.50213e+09	−0.000412490	0.0471572	0	0	0	0	0	0
901	950	1	−5.46384e+09	−0.000364589	0.0416744	0	0	0	0	0	0
977	977	1	−2.78948e+09	−0.000314466	0.0340743	0	0	0	0	0	0
951	1000	1	−1.16140e+09	−0.000121150	0.0131232	0	0	0	0	0	0
1026	1026	1	−4.35772e+09	−0.000276365	0.0316046	0	0	0	0	0	0
1032	1032	1	−5.70913e+09	−0.000374537	0.0405736	0	0	0	0	0	0
1001	1050	1	−4.29115e+09	−0.000302415	0.0327572	0	0	0	0	0	0

and TORR (1985), and TOBISKA and BARTH (1990).

Prior to performing the multiple linear regressions between the proxy datasets and the EUV irradiances, the proxy datasets are first searched for missing data followed by the insertion of a cubic spline interpolated value at the missing days. In practice, the $F_{10.7}$ has very few missing data points with exceptions in solar cycles 18 and 19. The He I 10,830 Å EW dataset contains a significant number of missing data points and the cubic spline is extensively used here. For ease of use in the model, the He I 10,830 Å EW data, originally in units of mÅ, are converted to an equivalent SME Lyman-α flux by the relationship

$$F_{\text{Lyman alpha}} = F_{\text{He I 10,830 EW}} \cdot 3.7784687 \times 10^{9} + 8.4031723 \times 10^{10} \quad (6)$$

in units of photons $\text{cm}^{-2}\,\text{s}^{-1}$. Equation (6) is used to create the $F_2(t)$ dataset mentioned above. The SME Lyman-α dataset contains values for all dates except one or two. The OSO 4, OSO 6, and AEROS A Lyman-α data contain no missing datapoints as a result of the digitizing method used to create the datasets from the published figures and, finally, the AE-E Lyman-α dataset contains a substantial number of missing days where cubic splined data values are used. The datasets of EUV irradiance, which contain missing data, are not splined. The correlations are then performed between the proxy data, which is splined in the above cases, and the existing, measured, unsplined EUV irradiances.

While calculating the correlations between the independent data and a particular EUV wavelength interval or discrete line, several constraints were imposed upon the calculations. First, all EUV datasets were weighted with the uncertainties published by the experimenters although, in most cases, the uncertainties in the data were increased based either upon discussions with the experimenters or upon a comparison with other datasets when more than two sets of measurements were available for similar levels of solar activity.

Next, below 30.0 nm a first-order approximation to a rocket spectrum was created for each of the 3 USC datasets (CARLSON *et al.*, 1984; OGAWA and JUDGE, 1986; OGAWA *et al.*, 1990). This was accomplished by scaling the August 1979 AFGL rocket flight spectrum described by VAN TASSEL *et al.* (1981) by the appropriate ratio so that the total spectrum between 5.0–57.5 nm equalled the total integrated flux value obtained by the USC experimenters. The uncertainty introduced by this approximation is certainly large even though the AFGL flight occurred under similar levels of solar activity. However, the resulting estimated flux values in this wavelength region for the USC rocket flights were almost always within ±50% of the model values which were derived only from a correlation with the AE-E dataset. Often the model vs estimated flux differences were within ±20%. These estimated rocket values were then used to scale the absolute magnitude of the AE-E data such that the model would best fit the estimated USC flux within a ±55% uncertainty range but still fall within the AE-E uncertainty range of ±35%. The exception using this technique below 30.0 nm was the calculation of the 25.6 nm irradiance which resulted in model values 65% higher than the AE-E values.

Between 1.8–5.0 nm, only the AFGL data as provided by the NSSDC were used in the correlation. It is possible that model fluxes in this range should be scaled upwards by as much as 50% for a first order approximation. Supporting this scaling is recent work by BARTH *et al.* (1988) and SISKIND *et al.* (1990) who, in analyzing NO in the lower thermosphere, suggest that the NSSDC values between 1.8–5.0 nm be raised in order to account for photoelectron flux needed to enhance the ionization of N_2.

Above 30.0 nm the same scaling technique which modifies the absolute value of the AE-E data was used such that the model matched the least uncertain of the measured intervals and lines of the 10 November 1988 and 20 June 1989 LASP rockets. In some cases described below, this technique was modified with additional constraints. All but a few of the model values were within ±10–50% of the AE-E flux for a given wavelength. The cases in which the comparisons were worse than this are those wavelength ranges which were forced to an absolute level by the continuum emission constraint described in the next paragraph. Above 30.0 nm the estimated USC data were not used in the determination of the absolute magnitude. However, in most cases, there were good to moderate agreements between the estimated USC data and the model where the scatter of differences ranged between ±5–75%. Except for the He II 30.4 nm emission, for which the AE-E dataset was given the most weight in order to best represent all the data, the USC estimates and model differences were attributable to greater weights given to the LASP narrowband spectrograph measurements or continuum emission constraints. The LASP rockets' measurement uncertainties varied by wavelength (see Table 1) and, for modelling purposes, the values given with those datasets were doubled to provide $\pm 2\sigma$ uncertainties.

An important empirical constraint related to the continuum emission was added to the model. For the three continua of He I (45.3–50.4 nm), H Lyman

(70.0–91.2 nm), and C I (91.3–105.0 nm) an empirical limitation was imposed in order to make adjacent longer wavelength interval boundaries produce an irradiance consistent with an increase relative to its neighbour in the preceding, shorter wavelength interval. The estimated value of the continuum flux in a wavelength interval for a given date was derived by scaling the reference continuum given by HINTEREGGER *et al.* (1981) in the SC21REFW spectrum by the ratio of Lyman-α and He I 10,830 Å EW on that date above their solar minimum values. This scaling philosophy is based upon the assumption that the continua irradiances in all three cases originate in the solar chromosphere. The modelled flux for wavelength intervals which include those continua were forced to match the expected scaled continua without regard for most discrete lines. In half of the cases, the model continua values were within ±20% or less of the rocket or AE-E data. The exceptions tended to be some of the emissions measured by the 1989 LASP rocket and AE-E, both of which had higher emission intensities by up to a factor of 2 than those derived from the model.

The model is constructed to take advantage of potentially new independent proxies such as the 530.3 nm coronal green line of Fe XIV. Possible new indices for chromospheric emission include the Mg II core-to-wing ratio R(Mg II cw) described by HEATH and SCHLESINGER (1986) and the Ca II K 1 Å index described by WHITE *et al.* (1990). The Fe XIV may complement the $F_{10.7}$ as a purely coronal index depending upon the results of further research. The Mg II and Ca II K index are both substitutes for Lyman-α when the latter is unavailable. TOBISKA and BOUWER (1989) give a relationship between Mg II and Lyman-α

$$F_{\text{Lyman alpha}} = R(\text{Mg II cw}) \cdot 1.785 \times 10^{12} - 1.515 \times 10^{12} \quad (7)$$

in photons $\text{cm}^{-2}\ \text{s}^{-1}$. WHITE *et al.* (1990) give a relationship between Ca II K and Lyman-α

$$F_{\text{Lyman alpha}} = \text{K}_{\text{index}} \cdot 108 - 6.92 \quad (8)$$

in units of $\times 10^{11}$ photons $\text{cm}^{-2}\ \text{s}^{-1}$.

Comparison of model and datasets

The independent datasets upon which this model is constructed are shown in Fig. 1. All proxies are corrected to 1 AU. The (a) SME Lyman-α is described by BARTH *et al.* (1990), the (b) He I 10,830 Å EW is described by HARVEY (1984), the (c) Ottawa $F_{10.7}$ daily flux is available from the World Data Center A and is described originally by COVINGTON (1948), and the (d) 81-day running mean value of $F_{10.7}$ is from the same sources as (c). The time-frame in all four panels is from 1 January 1962 to 31 December 1989. Units in the time axis are in days. The maxima of solar cycles 20 and 21 can be seen in these panels as well as the rise of cycle 22. In addition, the 27-day solar rotational modulations are observed.

Selected model and data discrete line and interval irradiances are shown in the time series Figs 2 and 3. These are some of the lines and intervals which contribute the greatest heating to the Earth's thermosphere as demonstrated by ROBLE (1987). Figure 2 shows the 15–19.9 nm coronal emission, the Fe XV 28.4 nm coronal line, the He II 30.4 nm chromospheric line, the 30.3–35 nm coronal emission (excluding Si XI at 30.3 nm), the He I 58.4 nm chromospheric line, and the H Lyman-β 102.6 nm chromospheric line. In each of the panels, the data are shown as solid lines and the model as dotted lines. USC estimated rocket flight data are shown as open diamonds while the LASP rocket data are shown as boxes. Each panel shows the time series in days, with biennial intervals labelled, from 1 January 1962 to 31 December 1989 where the flux is in units of photons $\text{cm}^{-2}\ \text{s}^{-1}$. The solar source regions and wavelength line or interval in Å is shown in each panel.

In Fig. 2, the coronal irradiances are modelled for the entire period from 1962 to 1989 since the $F_{10.7}$ exists for the entire period. The chromospheric irradiances in this figure have limited representation in 1968, 1969, and late 1974 to early 1976 but have daily values starting in late 1976. OSO 4 and OSO 6 measured Lyman-α in 1968 and 1969, respectively, while He I 10,830 Å EW measurements exist beginning in late 1974.

In Fig. 3, each panel shows the same emission ranges or lines as in Fig. 2. The AE-E data is again shown as a solid line and the model as a dotted line for 500 days beginning 10 August 1977. This figure compares data with the model during the rise of solar cycle 21. One notes that the relative magnitude of variation of the model compared to the data for both 27-day solar rotational and 11-year solar cycle timeframes are similar. Additionally, the coefficients of linear correlation with the independent term ($F_{1\text{-}4}$) are shown in each panel.

Three representative model spectra are shown in Fig. 4 for low, moderate, and high solar activity. The first panel in Fig. 4 shows the modelled spectrum for 26 November 1985 (85330 in the year-day format) during low solar activity when the $F_{10.7} = 70$. The modelled spectrum for 10 November 1988 (88315) is shown in the second panel for the time of the LASP rocket flight when $F_{10.7} = 148$ during moderate

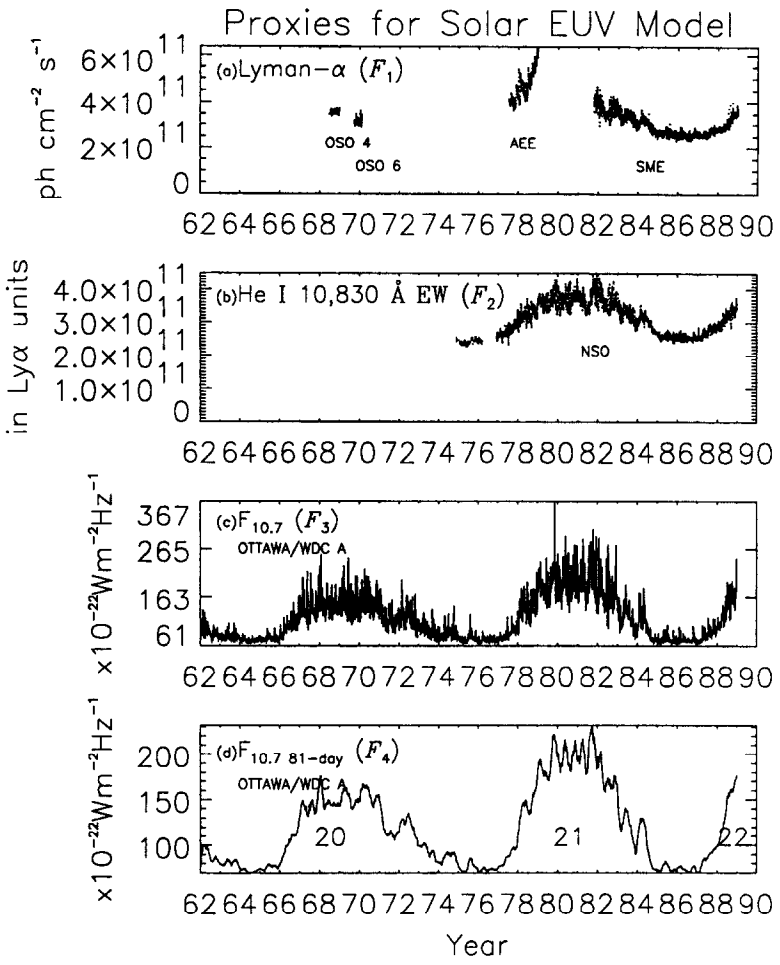

Fig. 1. Four datasets used as proxies for modelled solar EUV flux. The time-frame extends from 1 January 1962 to 31 December 1989 and units of flux are given in the ordinate labels. (a) Lyman-α, (b) He I 10,830 Å EW scaled to Lyman-α values by equation (6), (c) daily Ottawa $F_{10.7}$, (d) 81-day mean $F_{10.7}$ with the solar cycle designation superimposed under the cycle maxima. Abscissa units are in years with biennial intervals labelled.

activity. The third panel shows the spectrum for 10 August 1982 (82222) during the USC rocket flight when $F_{10.7} = 210$ during high solar activity. The range of flux covers five orders of magnitude; discrete lines as well as continua are apparent. The model spectra was created by using the SC21REFW reference spectrum, scaling it's data to the modelled flux values, and superimposing the modelled discrete lines onto the spectrum. The total integrated flux between 50–575 Å is also shown in each panel.

Finally, Fig. 5 is mostly based upon OGAWA *et al.* (1990) and shows the total integrated flux between 5.0–57.5 nm for eighteen rocket flights including the three USC experiments. In Fig. 5, the total integrated flux is compared to $F_{10.7}$ on the date of the rocket flight. Superimposed upon Fig. 5 are the results of several model runs for a variety of solar activity conditions. The modelled data-points are shown as filled circles without error bars. During low, moderate, and high solar conditions, the model reproduces very well the observed integrated solar flux. The dates of the models runs are 79050 (1979, day 50), 79226, 79314, 82222, 83228, 85330, 88298, and 88315 which correspond to high activity days, low activity days, or dates of rocket flights.

As noted earlier, there has been discussion in the

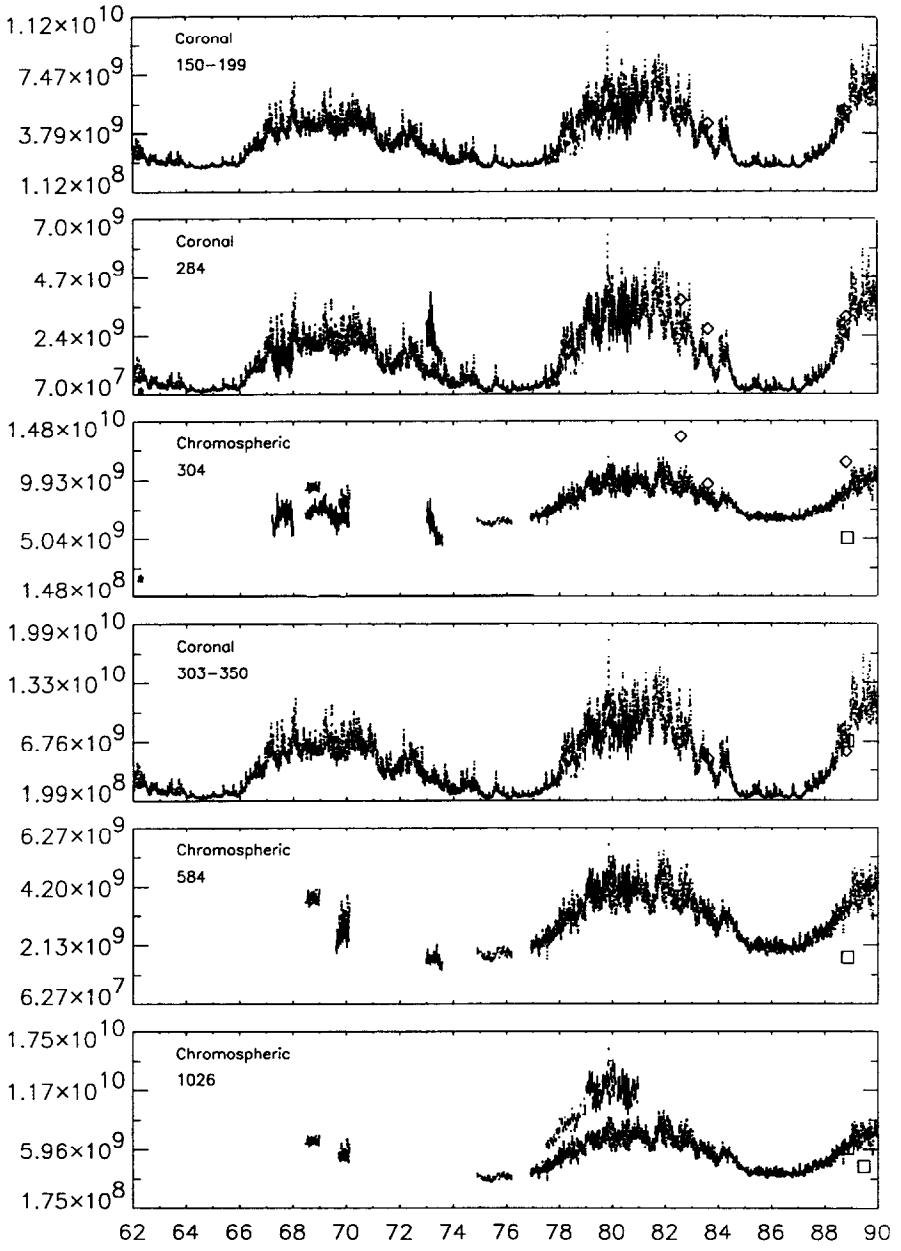

Fig. 2. Model 15–19.9 nm coronal emission, 28.4 nm coronal line, 30.4 chromospheric line, 30.3–35 nm coronal emission, 58.4 nm chromospheric line, and 102.6 nm chromospheric line values are shown as dotted lines compared with satellite (solid line) and rocket (USC are diamonds and LASP are boxes) data. The time scale on the abscissa is days beginning 1 January 1962 to 31 December 1989 with biennial intervals labelled. The flux values on the ordinate are in units of photons $cm^{-2} s^{-1}$ for all panels.

literature regarding the magnitude of the integrated flux values during low solar activity when $F_{10.7}$ is in the low 70s. One argument suggests that low solar activity total integrated flux should be higher by a factor of $1\frac{1}{2}$–2 based upon (1) calculations of the solar flux needed to produce measured photoelectron fluxes and (2) the extrapolation of a line through the low uncertainty USC measurements. The other argument

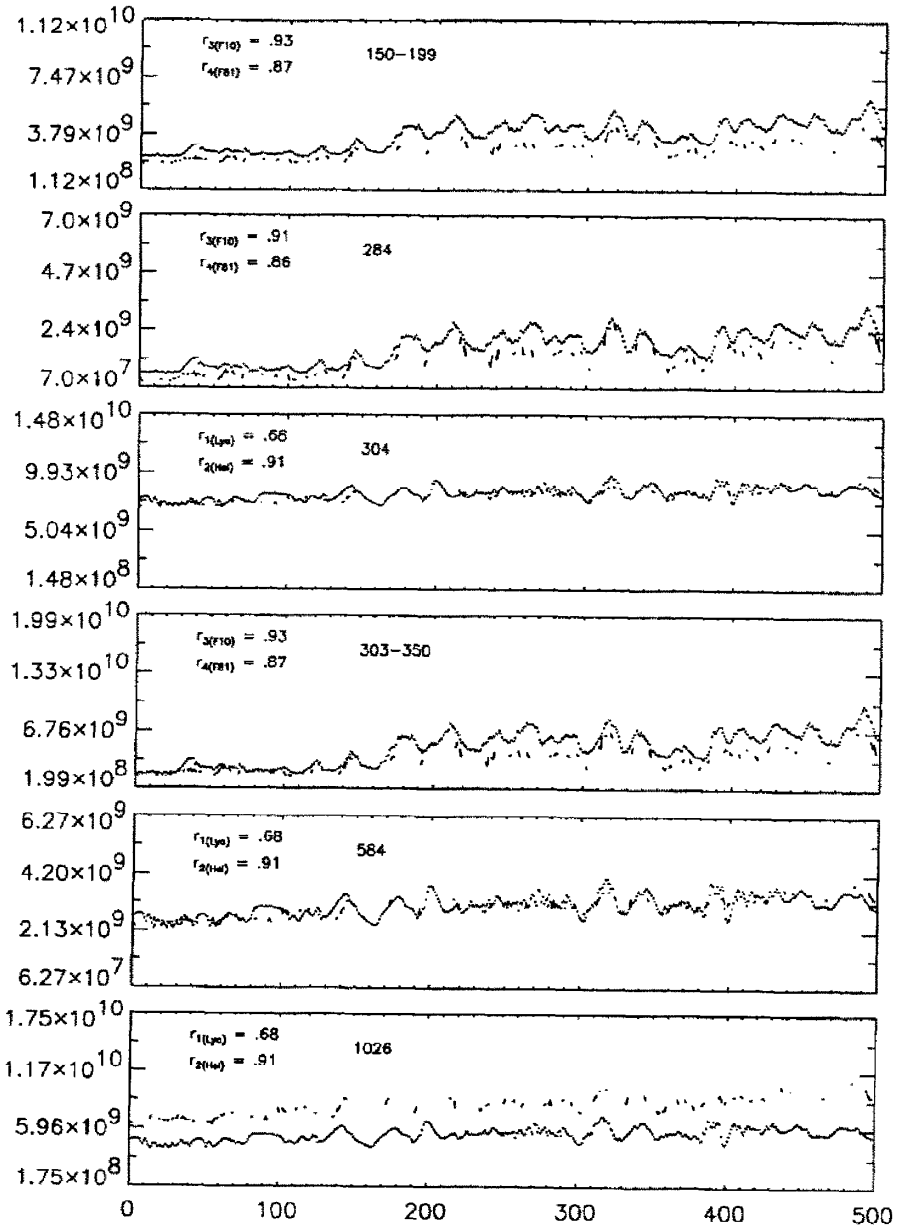

Fig. 3. Model flux (dotted lines) for the same lines and ranges as shown in Fig. 2 (labelled in Å) are compared with AE-E data (solid lines with missing data not plotted) for 500 days beginning 10 August 1977. The 27-day solar rotational features are apparent in both the model and dataset. The flux values on the ordinate are in units of photons cm^{-2} s^{-1} for all panels. Each panel also includes the derived linear correlation coefficients between the data and proxies.

notes that (1) three separate rocket flights measured consistent flux levels for low solar activity and (2) the 5.0–57.5 nm range contains a substantial amount of chromospheric irradiance which should vary non-linearly with $F_{10.7}$ by analogy to the Lyman-α, Mg II, and He I 10,830 comparisons with $F_{10.7}$. Since the model uses two of these three chromospheric indices, it is not surprising that the model (1) shows a non-

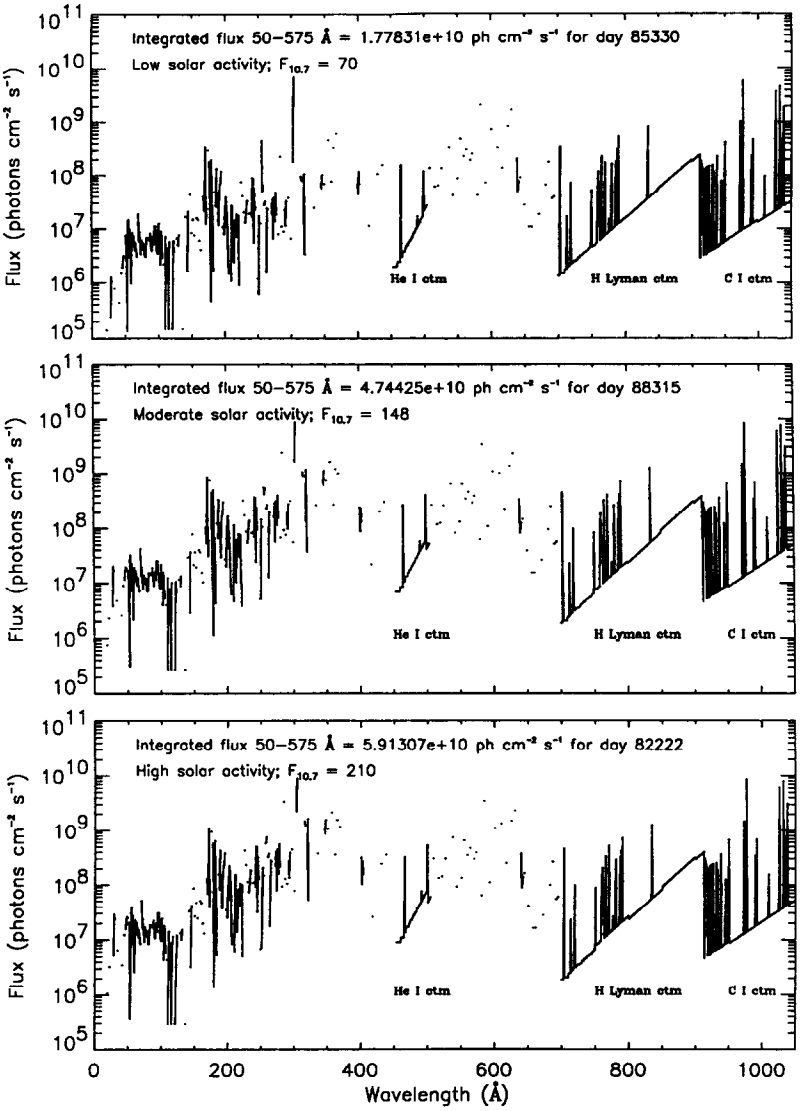

Fig. 4. The model solar EUV spectrum for 26 November 1985 (low solar activity), 10 November 1988 (moderate activity), and 10 August 1982 (high activity) are shown in three panels. The total integrated flux between 5.0–57.5 nm is 17.8×10^9 photons cm^{-2} s^{-1} for the November 1985 case, 47.4×10^9 photons cm^{-2} s^{-1} for the November 1988 case, and 59.1×10^9 photons cm^{-2} s^{-1} for the August 1982 case. The He I continuum is visible between 450–504 Å, the H Lyman continuum is between 700–912 Å, and the C I continuum is between 913–1050 Å in each panel. Discrete emission lines rise considerably higher than the continua. The modelled spectrum is based on the wavelength ranges of the SC21REFW spectrum and contains missing lines.

linear relationship with $F_{10.7}$ during low solar activity, (2) does not follow a direct extrapolation from moderate levels of solar activity, and (3) reproduces flux consistent with rocket data. The three low activity rocket datasets were not used directly in the model derivation but did indirectly affect the model to the extent that they were used in calibrating the AE-E EUV flux. However, it is possible that only the flux levels in wavelengths shortward of 25.0 nm need to be increased over the AE-E values while the irradiance above 25.0 nm does not need to be increased substantially. This combination allows increased photo-

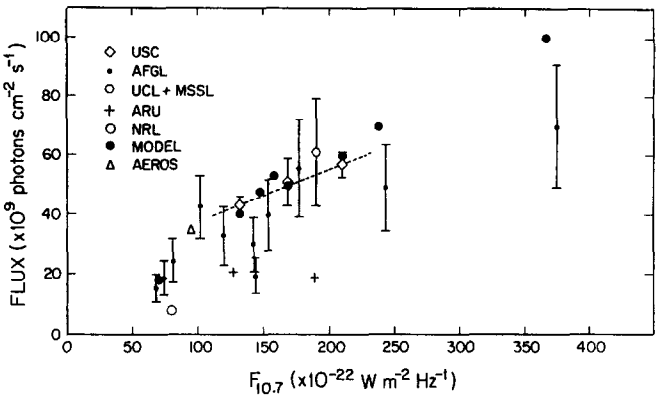

Fig. 5. The total integrated solar EUV flux between 5.0–57.5 nm as shown by OGAWA *et al.* (1990). Organizations which made individual rocket measurements are described in that reference. The USC data have the lowest uncertainty and are denoted by diamonds. The model values for a variety of levels of solar activity, as indicated by $F_{10.7}$ in the abscissa, are shown as filled circles with no error bars. See text for dates. An additional data point has been added with the AEROS A satellite measurement on 19 January 1973 when $F_{10.7} = 95$ which had an integrated flux of $34.6 \times 10^9 \pm 20\%$ described by SCHMIDTKE (1976).

electron production yet maintains a non-linear relationship with $F_{10.7}$ during low solar activity. The controversy remains an open question and demonstrates the importance of obtaining well calibrated solar EUV measurements during the next solar minimum in the mid-1990s.

CONCLUSIONS

The present solar EUV irradiance model was developed as an extension and revision of the SERF2 model. The 39 wavelength intervals or discrete lines between 1.8–105.0 nm are modelled as either chromospheric or coronal irradiances which vary over time with solar rotational or longer-term solar dynamical periodicities including the 11-year solar cycle. The modelled flux is representative of an average full-disk EUV irradiance on a given date at 1 AU at the top of the atmosphere. The model was constructed particularly for use in aeronomical calculations. The daily modelled spectrum can be used in a variety of formats, including broadband integrated flux in the 5.0–57.5 nm range, as 39 wavelength intervals and lines, or at a resolution of 1–2 Å with divisions identical to those of the SC21REFW reference spectrum.

The modelling technique utilizes two independent datasets for each of the chromospheric and coronal irradiances within a multiple linear regression algorithm which allows for the weighting of each EUV dataset according to instrumental uncertainty. Uncertainties were utilized in the derivation of the model. An empirical function incorporated into the model allows for the calculation of an irradiance even if only one independent term exists.

The present work is an improvement over SERF1 in its (1) ability to distinguish between chromospheric and coronal irradiance variations outside the AE-E time-frame and (2) self-consistency with the datasets which were used to derive the model. Improvements over SERF2 include (1) the ability to reproduce the same relative magnitude of variation over 27-day solar rotational and 11-year solar cycle time periods as the datasets for all wavelengths, (2) the ability to incorporate new datasets and/or independent proxies as they become available, and (3) the extension of the model beyond the SME Lyman-α timeframe. The model can be extended even further in time (forward and possibly backward for the chromospheric irradiances) as ground-based and/or satellite measurements of the proxies continue to be made.

Future improvements in the modelling of solar EUV irradiance will come with increased satellite and rocket measurements in this part of the spectrum at a variety of levels of solar activity. New measurements of the short wavelength solar EUV during solar minimum conditions in the mid-1990s, particularly of the integrated flux and the discrete lines down to 1.8 nm, would certainly contribute to resolving open questions regarding existing models and data. Narrowing the model uncertainty may also be possible through the use of improved or new independent proxies. Finally, short-term solar EUV flux prediction may soon be possible as the evolution and decay of solar active regions are better understood and this information is incorporated into the solar EUV models.

Acknowledgements—This research was supported by the US Army Research Office (USARO) and the National Science Foundation (NSF) through the following grants: USARO DAAL03-89-K-0057 and NSF ATM-8900145. Several datasets were graciously provided. The He I 10,830 Å EW data was provided by J. Harvey. These NSO/Kitt Peak data are produced cooperatively by NSF/NOAO, NASA/GSFC and NOAA/SEL. G. Rottman of LASP/University of Colorado provided the SME Lyman-α data. G. Fruth of the University of California at Berkeley digitized the published data of the OSO 1, 3, 4, 6 and the AEROS A data. The NSSDC provided the AE-E and August 1979 AFGL rocket datasets. T. Woods provided the 1988 and 1989 LASP sounding rockets' data. This model is available in digital form, including all coefficients and proxy datasets, from the NSSDC and WDC A.

REFERENCES

Barth C. A., Tobiska W. K., Rottman G. J. and White O. R.	1990	Comparison of 10.7 cm radio flux with SME solar Lyman alpha flux. *Geophys. Res. Lett.* **17,** 571–574.
Barth C. A., Tobiska W. K., Siskind D. E. and Cleary D. D.	1988	Solar terrestrial coupling: low-latitude thermospheric nitric oxide. *Geophys. Res. Lett.* **15,** 92–94.
Bevington P. R.	1969	Data reduction and error analysis for the physical sciences. McGraw-Hill, New York.
Carlson R. W., Ogawa H. S., Phillips E. and Judge D. L.	1984	Absolute measurements of the extreme UV solar flux. *Appl. Opt.* **23,** 2327–2332.
Chapman R. D. and Neupert W. M.	1974	Slowly varying component of extreme ultraviolet solar radiation and its relation to solar radio radiation. *J. geophys. Res.* **79,** 4138–4148.
Covington A. E.	1948	Solar noise observations on 10.7 centimeters. *Proc. of the I.R.E.* **36,** 454–457.
Donnelly R. F. and Pope J. H.	1973	The 1–3000 Å solar flux for a moderate level of solar activity for use in modeling the ionosphere and upper atmosphere. NOAA Technical Report ERL 276-SEL 25, Boulder.
Feng W., Ogawa H. S. and Judge D. L.	1989	The absolute solar soft X-ray flux in the 20–100 Å region. *J. geophys. Res.* **94,** 9125–9130.
Harvey J.	1984	Helium 10830 Å irradiance: 1975–1983. In Solar Irradiance Variations on Active Region Time Scales, B. LaBonte, G. Chapman, H. Hudson and R. Wilson (eds). NASA CP-2310, 197–211.
Heath D. F. and Schlesinger B. M.	1986	The Mg 280 nm doublet as a monitor of changes in Solar ultraviolet irradiance. *J. geophys. Res.* **91,** 8672–8682.
Heroux L. and Hinteregger H. E.	1978	Aeronomical reference spectrum for solar UV below 2000 Å. *J. geophys. Res.* **83,** 5305–5308.
Hinteregger H. E.	1976	EUV fluxes in the solar spectrum below 2000 Å. *J. atmos. terr. Phys.* **38,** 791–806.
Hinteregger H. E., Fukui K. and Gilson B. R.	1981	Observational, reference and model data on solar EUV, from measurements on AE-E. *Geophys. Res. Lett.* **8,** 1147–1150.
Hinteregger H. E., Hall L. A. and Schmidtke G.	1965	Solar XUV radiation and neutral particle distribution in July 1963 thermosphere. *Space Res.* **V,** 1175–1190.
Lean J.	1990	A comparison of models of the Sun's extreme ultraviolet irradiance variations. *J. geophys. Res.* **95,** 11933–11944.
Lean J. L.	1987	Solar ultraviolet irradiance variations: a review. *J. geophys. Res.* **92,** 839–868.
Link R., Gladstone G. R., Chakrabarti S. and McConnell J. C.	1988	A reanalysis of rocket measurements of the ultraviolet dayglow. *J. geophys. Res.* **93,** 14631–14648.
Neupert W. M., Behring W. E. and Lindsay J. C.	1964	The solar spectrum from 50 Å to 400 Å. *Space Res.* **IV,** 719–729.
Ogawa H. S., Canfield L. R., McMullin D. and Judge D. L.	1990	Sounding rocket measurement of the absolute solar EUV flux utilizing a silicon photodiode. *J. geophys. Res.* **95,** 4291–4295.
Ogawa H. S. and Judge D. L.	1986	Absolute solar flux measurements shortward of 575 Å. *J. geophys. Res.* **91,** 7089–7092.
Richards P. G. and Torr D. G.	1984	An investigation of the consistency of the ionospheric measurements of the photoelectron flux and solar EUV flux. *J. geophys. Res.* **89,** 5625–5635.

ROBLE R. G. 1987 Solar cycle variation of the global mean structure of the thermosphere, in Solar Radiative Output Variation, NCAR, Boulder, Proceedings of a Workshop November 9–11, 1–24.

ROBLE R. G. and SCHMIDTKE G. 1979 Calculated ionospheric variations due to changes in the solar EUV flux measured by the AEROS spacecraft. *J. atmos. terr. Phys.* **41,** 153–160.

SAHA M. N. 1937 On the action of ultra-violet sunlight upon the upper atmosphere. *Proc. Roy. Soc. London A* **160,** 155–173.

SCHMIDTKE G. 1976 EUV indices for solar-terrestrial relations. *Geophys. Res. Lett.* **3,** 573–576.

SCHMIDTKE G. 1981 Solar irradiance below 120 nm and its variations. *Solar Phys.* **74,** 251–263.

SCHMIDTKE G. 1984 Modelling of the solar extreme ultraviolet irradiance for aeronomic applications. In Handbuch der Physik XLIX/7, Geophysics III, Part VII, ed. S. FLÜGGE. Springer-Verlag, Berlin, 1–55.

SCHMIDTKE G., RAWER K., BOTZEK H., NORBERT D. and HOLZER K. 1977 Solar EUV photon fluxes measured aboard Aeros A. *J. geophys. Res.* **82,** 2423–2427.

SISKIND D. E., BARTH C. A. and CLEARY D. D. 1990 The possible effect of solar soft X rays on thermospheric nitric oxide. *J. geophys. Res.* **95,** 4311–4317.

TIMOTHY A. F. and TIMOTHY J. G. 1970 Long-term variations in the solar helium II—Lyman alpha line. *J. geophys. Res.* **75,** 6950–6958.

TIMOTHY J. G. 1977 The solar spectrum between 300 and 1200 Å, in *The Solar Output and its Variation*, ed. O. R. WHITE, Colorado Associated University Press, Boulder, 133–150.

TOBISKA W. K. 1988 A Solar Extreme Ultraviolet Flux Model, Ph.D. thesis, Department of Aerospace Engineering, University of Colorado, Boulder.

TOBISKA W. K. 1989 Modeled solar EUV flux during Equinox Transition Study: September 17–24, 1984. *J. geophys. Res.* **94,** 17017–17020.

TOBISKA W. K. 1990 SERF2: A solar extreme ultraviolet flux model, Earth and Planetary Atmospheres Group, Space Sciences Laboratory, University of California, Berkeley, Contribution 9.

TOBISKA W. K. and BARTH C. A. 1990 A solar EUV flux model. *J. geophys. Res.* **95,** 8243–8251.

TOBISKA W. K. and BOUWER S. D. 1989 Intermediate-term variations of chromospheric and coronal solar flux during high solar cycle 21 activity. *Geophys. Res. Lett.* **16,** 779–782.

TORR M. R. and TORR D. G. 1985 Ionization frequencies for solar cycle 21: revised. *J. geophys. Res.* **90,** 6675–6678.

TORR M. R., TORR D. G., ONG R. A. and HINTEREGGER H. E. 1979 Ionization frequencies for major thermospheric constituents as a function of solar cycle 21. *Geophys. Res. Lett.* **6,** 771–774.

VAN TASSEL R. A., MCMAHON W. J. and HEROUX L. 1981 Rocket data of solar EUV flux, thermospheric electron flux, and N_2 second-positive airglow emission. *Environ. Res. Pap., 737, AFGL-TR-81-011*, Air Force Geophys. Lab., Hanscom Air Force Base, Mass.

WHITE O. R., ROTTMAN G. J. and LIVINGSTON W. C. 1990 Estimation of the solar Lyman alpha flux from ground based measurements of the Ca II K line. *Geophys. Res. Lett.* **17,** 575–578.

WINNINGHAM J. D., DECKER D. T., KOZYRA J. U., JASPERSE J. R. and NAGY A. F. 1989 Energetic (>60 eV) atmospheric photoelectrons. *J. geophys. Res.* **94,** 15335–15348.

WOODGATE B. E., KNIGHT D. E., URIBE R., SHEATHER P., BOWLES J. and NETTLESHIP R. 1973 Extreme ultraviolet line intensities from the Sun. *Proc. Roy. Soc. London, A,* **332,** 291–309.

WOODS T. N. and ROTTMAN G. J. 1990 Solar EUV irradiance derived from a sounding rocket experiment on November 10, 1988. *J. geophys. Res.* **95,** 6227–6236.